RESEARCH ARTICLE | JANUARY 03 2025

Collision characteristics of neutral and highly charged droplets in uniform electric fields

Ming Zhang (张明) ; Zhiwen Yang (杨志文); Chuan Li (李传) ; Jiawei Li (李家玮); Dingchen Li (李丁晨) ; Qixiong Fu (傅琦雄); Kexun Yu (于克训)

Physics of Fluids 37, 012005 (2025)
https://doi.org/10.1063/5.0247783

Physics of Fluids ARTICLE pubs.aip.org/aip/pof

Collision characteristics of neutral and highly charged droplets in uniform electric fields

Cite as: Phys. Fluids **37**, 012005 (2025); doi: 10.1063/5.0247783
Submitted: 8 November 2024 · Accepted: 11 December 2024 ·
Published Online: 3 January 2025

View Online Export Citation CrossMark

Ming Zhang (张明),[1] Zhiwen Yang (杨志文),[1] Chuan Li (李传),[1,a)] Jiawei Li (李家玮),[1] Dingchen Li (李丁晨),[2] Qixiong Fu (傅琦雄),[1] and Kexun Yu (于克训)[1]

AFFILIATIONS

[1]International Joint Research Laboratory of Magnetic Confinement Fusion and Plasma Physics, State Key Laboratory of Advanced Electromagnetic Technology, School of Electrical and Electronic Engineering, Huazhong University of Science and Technology, Wuhan 430074, China

[2]Department of Building Environment and Energy Engineering, The Hong Kong Polytechnic University, Hong Kong 999077, China

[a)]Author to whom correspondence should be addressed: lichuan@hust.edu.cn

ABSTRACT

Droplet collision and growth are common phenomena. While charge and electric fields can promote the droplet collision process, the impact of field intensity and high charge on droplet collision characteristics, as in thunderclouds, is not well understood. This paper presents a trajectory model to study the collision characteristics of a neutral droplet and a charged droplet with varying amounts of charge under various electric field intensities. The findings reveal a transition stage in collision efficiency as the electric field E increases, related to droplet size variation. During this transition stage (about $E = 7.5 \times 10^2$ V·m^{-1} to 7.5×10^4 V·m^{-1}), there is a peak in the collision efficiency of highly charged and neutral droplets as the neutral droplet size increases. Conversely, at other electric fields (near 10^2 V·m^{-1} and between 7.5×10^4 V·m^{-1} and 10^7 V·m^{-1}), a larger neutral droplet is advantageous for enhancing the collision efficiency, increasing the collision probability. Throughout the range from 10^2 V·m^{-1} to 10^7 V·m^{-1}, a larger neutral droplet is beneficial for enhancing the collision kernel, raising the collision frequency. An increase in charge significantly enhances both collision efficiency and kernel. For a micrometer-sized charged-neutral droplet pair, collision efficiency initially decreases (disturbance effect) and then slightly rises to about 1.0 (inertial effect) with the electric field at a constant droplet size ratio. In addition, the impact of droplet size on collision characteristics was investigated, and the collision characteristics of two neutral droplets were compared. The results deepen our understanding of the internal physical processes of cloud droplet collisions under varying electric fields and charge conditions (especially high charges) and provide guidance for applications like electrostatic defogging, charged particle catalyzed rainfall, and fog collection.

I. INTRODUCTION

The charged particle clusters generated after gas ionization can form low-temperature, high-temperature plasma,[1,2] etc. The interaction between charged particles and polar water molecules can charge the droplets, leading to various distinct characteristics. Recently, the effects of electric charge and electric field on droplet collisions have been widely studied, such as electrostatic defogging,[3,4] charged particles catalyze artificial rainfall,[5,6] and the impact of charge and atmospheric electric field on droplet collisions.[7,8] Under natural conditions, the key issue in the rain formation or fog dissipation is the efficient formation of a considerable number of large droplets above the critical size (20–25 μm).[9] However, the average particle size of droplets in the air mainly ranges from sub-micron to 10 μm.[10] Natural fog and clouds often persist over extended periods.

It is well known that in thunderstorm clouds, rain can form rapidly, and a significant factor in this process is the influence of the background electric field and a large amount of charge. Prior studies have also shown that the effects of charge and electric fields can significantly promote the collision and growth of droplets.[11–14] Cruzat and Jerez-Hanckes[15] introduced an external electric field into their experimental device, proving that applying electric power to droplets can substantially alter their motion and augment fog water collection. Khain *et al.*[16] achieved accelerated droplet collision by seeding charged droplets with different charges to enhance the effect of precipitation and fog removal. Damak and Varanasi[17] and Li *et al.*[18,19] introduced an external electric field and inserted space charge, discovering that the combined influence of these two factors can effectively facilitate fog dissipation or water collection. However, these studies are more of a

macroscopic effect, and the specific internal action laws of charge and electric field on droplet collision and growth remain to be elucidated.

Moreover, Semonin and Plumlee[20] found through numerical simulation that only when the charge is greater than[10–16] C or the electric field intensity exceeds 900 V·cm^{-1}, the collision efficiency will be affected. However, the disturbance of the fluid around the droplet was not considered in the study. Wang *et al.*[21] observed the phenomenon of sub-micron droplets growing to large droplets above[25] μm in corona discharge experiments, which was mainly due to the uneven distribution of charge and electric field significantly enhanced the collision between droplets. Yet, the internal action mechanism behind the uneven distribution of charge and electric field remains unclear.

The charge of droplets in thunderclouds can reach quite high levels, potentially approaching the Rayleigh limit charge at which the droplet is on the verge of breaking up due to repulsion between charges.[24] However, previous studies on the internal action mechanism of droplet collision and growth influenced by charge and electric fields generally focused on low charge levels and only considered fixed charge amounts. For example, in the simulation study by Guo and Xue[7] on the impact of charge and electric fields on droplet collisions, the charge levels ($q = 0$ or $\pm 32r^2$, q in units of elementary charge, and r in units of μm) are far below the Rayleigh limit, such as a charge ratio $CR = Q/Q_{\mathrm{Ray}} = 8 \times 10^{-4}$ for charged droplets with a radius of 10 μm. Moreover, in the study by Li *et al.*[22] on the collision characteristics of two droplets under different uniform electric fields, the charge levels of the charged droplets [$q = 12\pi\varepsilon_0 r^2 E\varepsilon_r/(\varepsilon_r + 2)$, r in units of m] are also low and fixed, such as a charge ratio $CR = 0.05$ for charged droplets with a radius of 10 μm. Additionally, the accuracy of the formula for calculating the mirror electric field force between droplets in Li's paper is relatively low, which may limit the generalizability of the findings. As shown in Fig. 1, at low charge (low CR), the calculated results of the mirror electric field force using the formula from Li *et al.*[22] and the high-precision formula from Davis,[23] respectively, are consistent, while at high charge, the difference gradually increases. It is necessary to use the high-precision calculation formula of electrostatic force to explore the neutral and highly charged droplets collision characteristics.

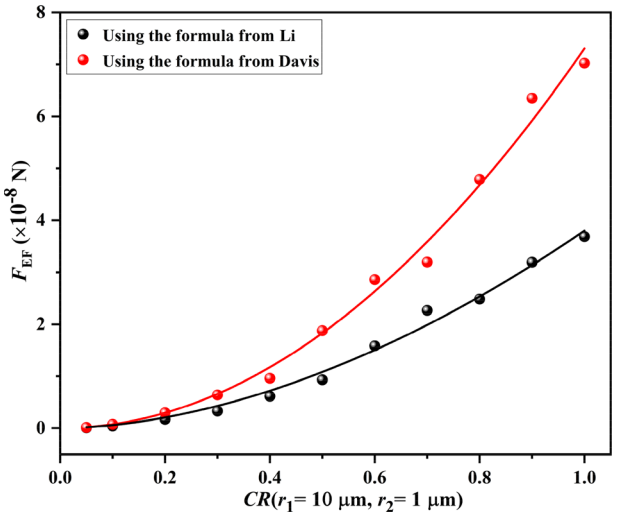

FIG. 1. The relation of the mirror electric field force F_{EF} with the charge ratio CR at the critical collision position. CR ($=Q/Q_{max}$) is the ratio of the charged droplet's actual charge to its maximum charge (Rayleigh limit charge Q_{Ray}). The black dots and red dots, respectively, represent the results obtained by using the mirror electric field force calculation formula from Li *et al.*[22] and Davis.[23] The curve in the figure is the fitted curve.

In summary, previous related studies have either focused on the macroscopic effects of high charge on droplet collision and growth or examined the collision characteristics of droplets with low (typically fixed) charge levels under an electric field. However, the maximum achievable charge that a droplet can achieve can approach the Rayleigh limit, and the charge it can carry is variable.[25] There is a lack of systematic research on highly charged droplet and neutral droplet collision problem under different electric fields and charges levels (especially high charges near the Rayleigh limit).

The electrostatic attraction between droplets is short-range,[26] and droplets with the same charge will repel each other at extended distances, while charged droplets and neutral droplets always attract each other.[12] Furthermore, while droplets carrying opposite polarity charges exhibit stronger attractive forces, intense initial collisions in practical application can rapidly deplete the droplet's net charge, reducing the net effect of charge on collision and growth.[16] In contrast, unipolar charges do not vanish due to collisions and can influence the whole process of droplet collision and growth. Therefore, neutral droplets tend to gather near charged droplets in localized regions of the external environment. Consequently, promoting the collision process between charged and neutral droplets is an important problem in the study of electrostatic fog removal and rain enhancement.

In this paper, we employ trajectory models that consider flow drag force ($\boldsymbol{F}_{\mathbf{D}}$), mirror electric field force ($\boldsymbol{F}_{\mathbf{EF}}$), gravity ($\boldsymbol{F}_{\mathbf{G}}$), and applied electric field force ($\boldsymbol{F}_{\mathbf{AE}}$) to compute collision efficiency and kernel. This approach permits a detailed analysis of how varying uniform electric fields and charges affect the collision characteristics of neutral and charged droplets. The electrostatic force between droplets is calculated using the high-precision calculation model established by Davis.[23]

II. MODEL BUILDING

A. Characterization of droplet charge and collision

In theory, insulating particles can carry arbitrary large charges. However, a droplet with a certain size cannot be charged beyond a certain maximum value Q_{max}, determined by the Rayleigh limit charge at which the droplet is on the verge of breaking up due to charge repulsion.[24] The specific expression of Rayleigh limit charge Q_{Ray} is as follows:[27]

$$Q_{max} = Q_{Ray} = 8\pi\sqrt{\varepsilon_0 \sigma_0 r^3}, \tag{1}$$

where ε_0 is the permittivity of air, σ_0 is the surface tension of water, and r is the radius of droplet. For example, with r values of 0.1, 1, and 10 μm, the corresponding QRay values are 6.4×10^{-16} C, 2.0×10^{-14} C, and 6.4×10^{-13} C, respectively.

In this study, the charge of a certain size of the charged droplet is $Q = (0 \sim 1)\ Q_{max}$. Meanwhile, the range of electric field strengths studied in this paper, from 10^2 V·m^{-1} to 10^7 V·m^{-1}, encompasses the atmospheric electric fields during fair weather (about 10^2 V·m^{-1}) and during thunderstorms.[9]

Figure 2 shows the relative motion between a centrally charged droplet and its surrounding neutral droplet under different force combinations. For a pair of droplets, each one will induce

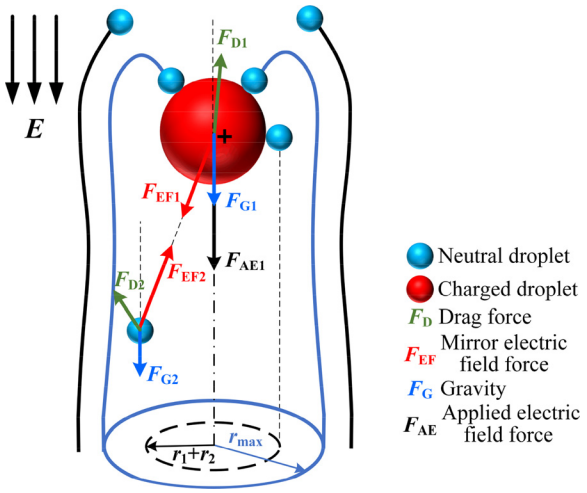

FIG. 2. Diagram of droplet collisions and forces between droplets under uniform electric field. r_1, r_2—radius of charged and neutral droplet and r_{max}—horizontal critical distance of droplets. The applied electric field $\boldsymbol{E}$ is vertically downward. Note that the mirror electric field force ($\boldsymbol{F}_{EF}$ in the figure) and the applied electric field force ($\boldsymbol{F}_{AE}$ in the figure) can be combined into the electrostatic force $\boldsymbol{F}_e$.

a flow field that interacts with the other. As the charged droplet falls, nearby small droplets tend to move along the streamlines of the flow field induced by the large droplet. Droplets collide with the charged droplet only when they have enough inertia or enough attractive force to cross the streamlines. The collision efficiency α is then defined as the ratio of the actual collisions over all possible collisions in the swept volume.[7] The collision kernel K is utilized to quantify the collision frequency of droplets with varying radii, expressed as the number of collisions per unit concentration, per unit volume, and per unit time,[28]

$$\begin{cases} \alpha = \dfrac{r_{max}^2}{(r_1+r_2)^2} \\ K = \alpha |\boldsymbol{V}_1 - \boldsymbol{V}_2| \pi (r_1+r_2)^2, \end{cases} \tag{2}$$

where r_{max} is the maximum horizontal distance between two droplets that can collide. r^1 and r_2 are the radius of charged and neutral droplets, respectively. $\boldsymbol{V}$ is the terminal velocity of the droplet. It is the steady-state velocity of the droplet relative to the fluid when no other droplets are present (no interaction from other droplets). Among them, the collision efficiency α can be interpreted as the likelihood of a collision occurring between two droplets.

B. Equation of droplet motion

In order to calculate the collision efficiency and collision kernel, the equations of motion need to be solved. Droplet motion depends mainly on the following forces: the flow drag force ($\boldsymbol{F}_D$), gravity ($\boldsymbol{F}_G$), and the electrostatic force ($\boldsymbol{F}_e$) due to droplet charge and the external electric field (the electrostatic force $\boldsymbol{F}_e$ consists of the mirror electric field force $\boldsymbol{F}_{EF}$ and the applied electric field force $\boldsymbol{F}_{AE}$). The equations of motion for a pair of droplets are as follows:

$$\begin{cases} \dfrac{d\boldsymbol{V}_1}{dt} = \dfrac{\boldsymbol{F}_{D1}}{m_1} + \mathbf{g} + \dfrac{\boldsymbol{F}_{e1}}{m_1} \\ \dfrac{d\boldsymbol{Y}_1}{dt} = \boldsymbol{V}_1 \\ \dfrac{d\boldsymbol{V}_2}{dt} = \dfrac{\boldsymbol{F}_{D2}}{m_2} + \mathbf{g} + \dfrac{\boldsymbol{F}_{e2}}{m_2} \\ \dfrac{d\boldsymbol{Y}_2}{dt} = \boldsymbol{V}_2, \end{cases} \tag{3}$$

where $\mathbf{g}$ is the gravitational acceleration, $\boldsymbol{V}$ is the velocity of the droplet relative to the fluid when there are no other droplets present, $\boldsymbol{Y}$ is the location of droplets, and m is the droplet mass, with $m = 4\pi r^3 \rho/3$.

Among them, the flow drag force ($\boldsymbol{F}_D$) of droplet in the air is expressed as[22]

$$\boldsymbol{F}_D = -\frac{C_D A \rho_{air}}{2C} |\boldsymbol{V} - \boldsymbol{u}| (\boldsymbol{V} - \boldsymbol{u}), \tag{4}$$

where C_D is the drag coefficient, A is the maximum cross section of droplet, ρ_{air} is the air density, C is the Cunningham correction coefficient, and $\boldsymbol{V}$ and $\boldsymbol{u}$ are the velocity of droplet and the flow velocity field induced by the droplet (disturbance velocity), respectively.

The Cunningham correction coefficient C is as follows:

$$\begin{cases} C = 1 + \left(1.257 + 0.4 \exp\left(-\dfrac{1.1}{K_n}\right)\right) K_n \\ K_n = \dfrac{21.55 \mu T^{0.5}}{r\, p}, \end{cases} \tag{5}$$

where μ is the air dynamic viscosity, r is the radius of droplet, and we set the air temperature at T = 293.15 K and the pressure p = 101.3 kPa in this study for the calculation of air dynamic viscosity.

This paper uses the superposition method to elucidate the hydrodynamic interactions between charged and neutral droplets,[29] assuming one droplet moves in the flow field induced by the other. The disturbance velocity $\boldsymbol{u}$ of a single droplet is computed using an improved superposition method and is expressed as follows:[30]

$$\boldsymbol{u}(\boldsymbol{d}, r, \boldsymbol{V}) = \left[\frac{3r}{4d} - \frac{3}{4}\left(\frac{r}{d}\right)^3\right] \frac{\boldsymbol{d}}{d^2} (\boldsymbol{V} \cdot \boldsymbol{d}) + \left[\frac{3r}{4d} + \frac{1}{4}\left(\frac{r}{d}\right)^3\right] \boldsymbol{V}, \tag{6}$$

where $\boldsymbol{d}$ is the position vector relative to the droplet center and r and $\boldsymbol{V}$ are the radius and terminal velocity of the droplet, respectively.

The disturbance velocities of the two droplets in the interacting flow field are as follows:

$$\boldsymbol{u}_1 = \boldsymbol{u}(\mathbf{Y}_1 - \mathbf{Y}_2, r_2, \boldsymbol{V}_2 - \boldsymbol{u}_2), \tag{7}$$

$$\boldsymbol{u}_2 = \boldsymbol{u}(\mathbf{Y}_2 - \mathbf{Y}_1, r_1, \boldsymbol{V}_1 - \boldsymbol{u}_1), \tag{8}$$

where $\boldsymbol{u}$ is the disturbance velocity of a single droplet when no other droplets are present. $\boldsymbol{Y}_1$, $\boldsymbol{Y}_2$, r_1, r_2, $\boldsymbol{V}_1$, and $\boldsymbol{V}_2$ are the locations, radii, and the terminal velocities of the two droplets, respectively. In conjunction with Eqs. (6)–(8), when calculating $\boldsymbol{u}_1$, the parameters $\boldsymbol{d}$, r, and $\boldsymbol{V}$ in Eq. (6) are substituted with $\boldsymbol{Y}_1 - \boldsymbol{Y}_2$, r_2 and $\boldsymbol{V}_2 - \boldsymbol{u}_2$, respectively. An analogous substitution is made for $\boldsymbol{u}_2$.

In the presence of a background electric field, the droplet exhibits an obvious polarization effect, where the positive and negative charges it carries migrate and rearrange to form an induced dipole moment.[31]

This induced dipole moment leads to interactions both between droplet (manifested as the mirror electric field force $\boldsymbol{F}_{\mathbf{EF}}$) and with the external electric field (manifested as the applied electric field force $\boldsymbol{F}_{\mathbf{AE}}$), collectively referred to as the electrostatic force $\boldsymbol{F}_{\mathbf{e}}$. Davis demonstrated an appropriate and high-precision computational method for the electrostatic force of two spherical conductors in a uniform external field, which is expressed as[23]

$$\begin{cases} F_{e1x} = E\cos\theta(Q_1+Q_2) - F_{e2x} \\ F_{e1y} = E\sin\theta(Q_1+Q_2) - F_{e2y} \\ F_{e2x} = \{4\pi\varepsilon_0 r_2^2 E^2(F_1\cos^2\theta + F_2\sin^2\theta) \\ \qquad + E\cos\theta(F_3Q_1 + F_4Q_2) \\ \qquad + \dfrac{1}{4\pi\varepsilon_0 r_2^2}(F_5Q_1^2 + F_6Q_1Q_2 + F_7Q_2^2)\} + EQ_2\cos\theta \\ F_{e2y} = \{4\pi\varepsilon_0 r_2^2 E^2 F_8\sin 2\theta + E\sin\theta(F_9Q_1 + F_{10}Q_2)\} + EQ_2\sin\theta, \end{cases} \tag{9}$$

where E is the applied electric field and θ is the angle between the electric field and the line connecting the centers of two droplets. ε_0 is the permittivity of air. r_1, Q_1, r_2, and Q_2 are the radius and charge of the two droplets, respectively. F_1 to F_{10} are a series of complicated dimensionless coefficients related to geometric parameters of r,[1] r_2 and the central distance R of the two droplets.

The initial velocities of the charged and neutral droplets are established as their respective terminal velocities, $\boldsymbol{V}_1$ and $\boldsymbol{V}_2$. The initial horizontal and vertical distances of the two droplets are $100(r_1+r_2)$ and $100r_1$, respectively. To approximate the condition of infinite distance, we initialize the disturbance velocities u_1 and u_2, along with the mirror electric field forces F_{EF1} and F_{EF2}, to zero.

To improve computing efficiency, the calculation of critical horizontal distance $r_{\max}$ adopts dichotomy. In the calculation, the actual horizontal distance x between two droplets is progressively halved until collision occurs. Then, $r_{\max}$ is the average of the horizontal distance corresponding to the last non-collision and the first collision event. The second-order Runge–Kutta method[32] is used to solve the equation of motion (3).

III. RESULTS AND DISCUSSION

A. Collision efficiency characteristic

To characterize the possibility of droplet collision under different electric fields, the collision efficiency was calculated. Figure 3 shows the effects of droplet size ratio β and charge ratio CR on the collision efficiency, with a constant charged droplet radius of 10 μm. As illustrated in Fig. 3, under the same electric field E and droplet size ratio β, the collision efficiency increases with the higher charge of the charged droplet. Under very low electric fields (E around 10^2 V·m^{-1}), the collision efficiency increases with β without an apparently upper limit. Under low electric fields (10^3 V·m^{-1} and 10^4 V·m^{-1}), the collision efficiency exhibits a peak value with the increase in β. When $E=10^3$ V·m^{-1}, the collision efficiency increases with β for low CR (below 0.5), but first increases and then decreases for high CR (above 0.7). When $E=10^4$ V·m^{-1}, the collision efficiency increases and then decreases with β across CR values from 0.1 to 1. Under high electric fields (10^5 to 10^7 V·m^{-1}), collision efficiency levels off with increasing β, reaching a plateau near 1.0 at $E=10^6$ V·m^{-1} and 10^7 V·m^{-1}. In fact, due to the droplet itself size, the collision efficiency plateau value slightly exceeds 1.0.

To further clarify collision efficiency variation rule under different electric fields and CR, Fig. 4 shows the relationship between collision efficiency and CR at the same droplet size ratio $\beta=0.1$. Under the same electric field, the collision efficiency of charged and neutral droplets increases with CR ($CR>0$). However, the increase is gentle and almost straight under high electric fields ($E=10^6$ V·m^{-1} and 10^7 V·m^{-1}). Under the same β, the collision efficiency of two neutral droplets ($CR=0$) increases with the electric field, but the value is very small when electric field $E<10^5$ V·m^{-1}. For charged droplet ($CR>0$) and neutral droplet, with the increase in electric field under the same CR, the collision efficiency first decreases and then slightly increases to around 1.0, which has a similar change rule to the study of Li *et al.*[22]

The droplet charge in Li's paper has a low value, for example, the corresponding charge ratio is about 0.05 when the radius of charged droplet is 10 μm. Further, this paper uses a formula with a higher accuracy than that in Li's paper to calculate the electrostatic force, and the studied droplet charge and size ranges are different, so there are some differences in the specific variation rules. In the case of low charge, a comparison between the outcomes calculated using the model in this paper and using the model from Li *et al.*[22] was conducted. The charged droplet charge is about 0.05 times the Rayleigh limit. As shown in Fig. 5, the calculation results of the two models at low charge have good consistency, which can explain the accuracy of the calculated model in this paper and the rationality of the calculation when the model is extrapolated to high charge.

Figure 5 also further explores the relationship between collision efficiency and electric field for different charge ratios CR at the same droplet size ratio β. It can be seen that the collision efficiency of charged and neutral droplets has a minimum value around $E=1.75\times10^5$ V·m^{-1} with the increase in E under each CR ($CR>0$). It can be seen more intuitively that with increasing electric field E, the collision efficiency first decreases and then slightly rises to about 1.0. However, for two neutral droplets ($CR=0$), the collision efficiency increases slowly at first and then increases rapidly with the increase in the electric field. When electric field $E>5\times10^5$ V·m^{-1}, the collision efficiency of two neutral droplets has exceeded that of charged droplet and neutral droplet.

To find out the internal reasons for the above-mentioned changes in collision characteristics, we calculated the drag force and electrostatic force of the neutral droplet before collision and critical collision (Fig. 6). Additionally, to further clarify the effects of electric field, charge, and droplet size on droplet collision characteristics, the relative motion trajectory of droplets was derived, as shown in Fig. 7.

Figure 6 shows that, under the same electric field, both the drag and electrostatic forces increase with neutral droplet size. Likewise, for the same neutral droplet size, both forces grow with increasing electric field strength. Among them, the electrostatic force at critical collision increases slowly with E, without a significant order of magnitude increase. At a relatively long distance before collision, the electrostatic force is much smaller than the drag force, but at close range (critical collision), when the electric field is below 10^6 V·m^{-1}, the electrostatic force exceeds the drag force. This further indicates that electrostatic force between droplets is a short-range interaction.

As we know, with the increase in E, the droplet has a more obvious polarization effect, causing the charge distribution to shift

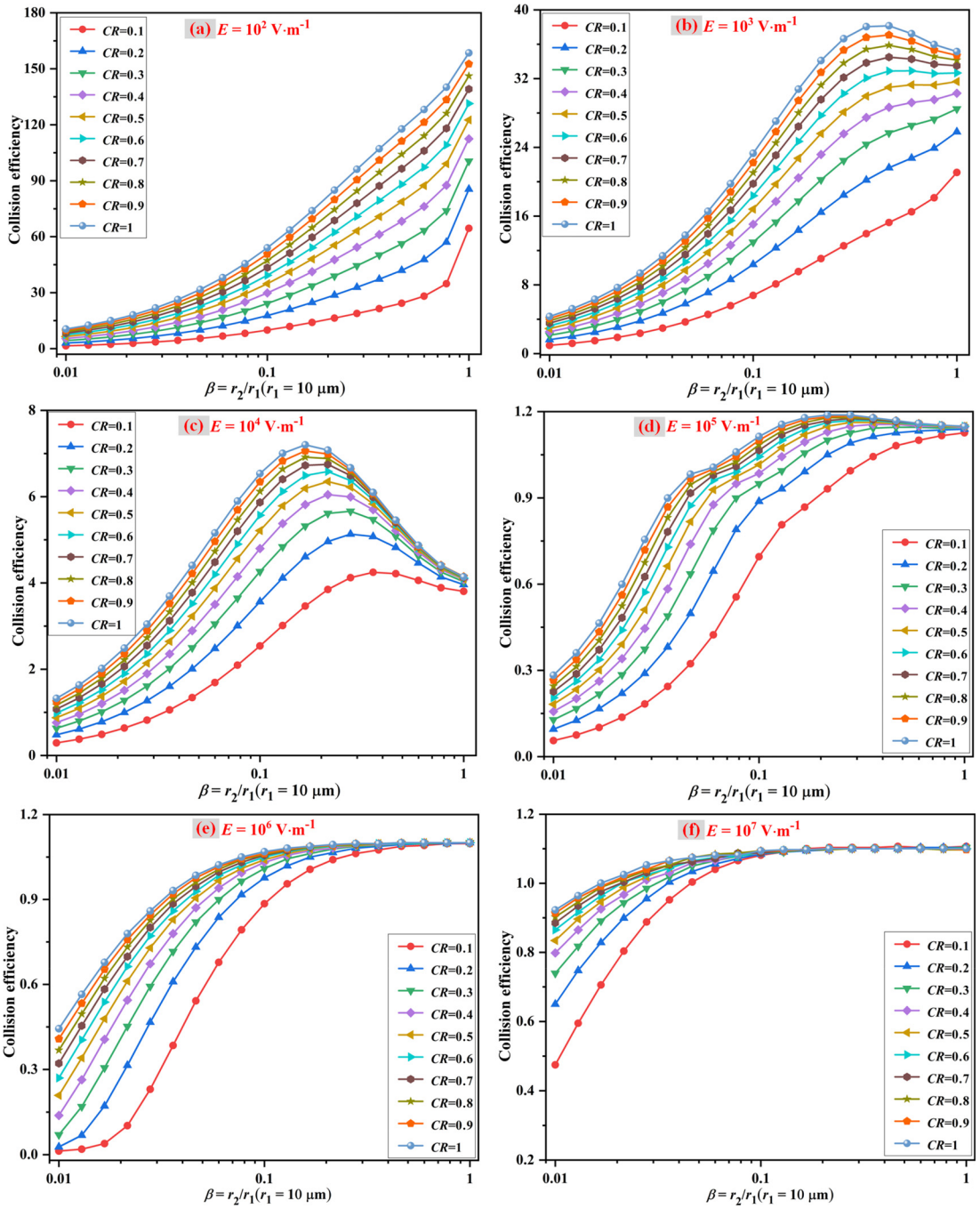

FIG. 3. Effects of β and CR on the collision efficiency, with charged droplet radius $r_1 = 10\ \mu m$. (a)–(f) The collision efficiency of a charged-neutral droplet pair when the electric field intensity E varying from 10^2 to 10^7 V·m^{-1}, respectively. Here, β ($=r_2/r_1$) is the radius ratio of neutral and charged droplets. CR ($=Q/Q_{max}$) is the ratio of the charged droplet's actual charge to its maximum charge (Rayleigh limit charge Q_{Ray}).

toward the ends and increasing the electrostatic force F_e on the neutral droplet. Additionally, with the increase in E, the applied electric field force F_{AE} on the charged droplet is significantly enhanced, accelerating its motion and increasing the disturbance around it. Moreover, with the increase in the neutral droplet size, the electrostatic attraction between the two droplet F_{EF} increases, further accelerating the charged droplet's motion and enhancing the disturbance. It can be seen from Eq. (4) that the drag force F_D

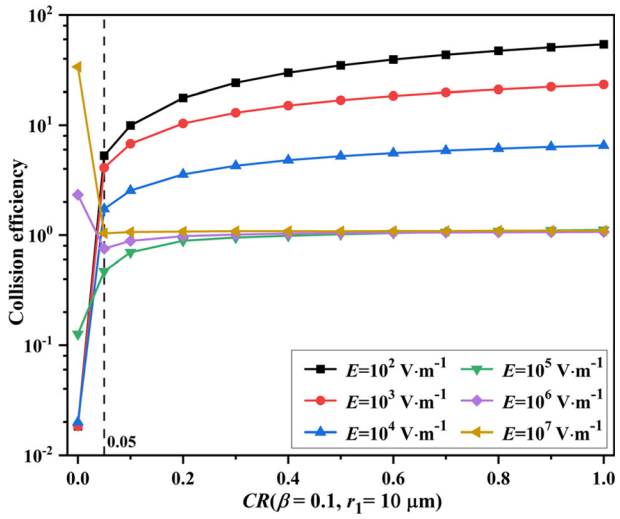

FIG. 4. Effects of *CR* on the collision efficiency, with a set of uniform electric fields varying from 10^2 to 10^7 V·m^{-1}, with two droplets radius $r_2 = 1$ μm and $r_1 = 10$ μm, respectively. *CR* ($=Q/Q_{max}$) is the ratio of the charged droplet's actual charge to its maximum charge Q_{Ray}.

of the neutral droplet will increase with its size (represented by the maximum cross section A in equation).

As can be seen from Fig. 7, with the increase in E at a small droplet size ratio, the dominant effect changes during the collision between charged droplet and neutral droplet. The electrostatic attraction effect dominates the collision process when E is low, while the inertial effect dominates the collision process when E is high. As mentioned above,

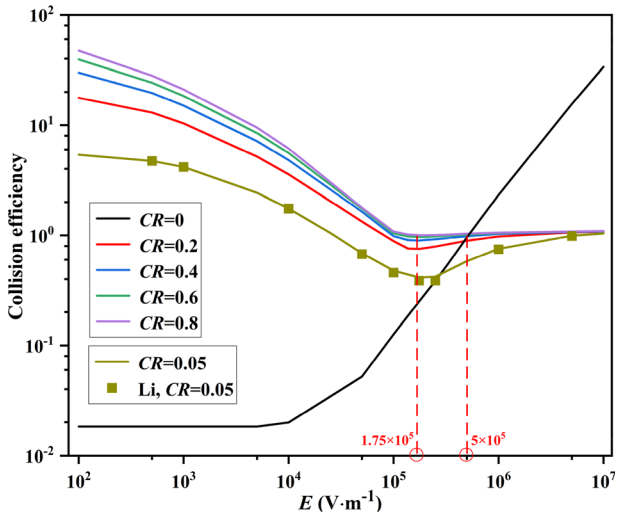

FIG. 5. Effects of electric field E on the collision efficiency, with a set of *CR* varying from 0 to 0.8, with $\beta = 0.1$ ($r_2 = 1$ μm and $r_1 = 10$ μm). Lines represent results from the model in this paper, while dots are from Li *et al.*'s model.[22] The charge of the charged droplet corresponding to the dots in the figure is consistent with that in Li *et al.* 's paper (about 0.05 times the Rayleigh limit). Here, β ($=r_2/r_1$) is the radius ratio of neutral and charged droplets. *CR* ($=Q/Q_{max}$) is the ratio of the charged droplet's actual charge to its maximum charge Q_{Ray}.

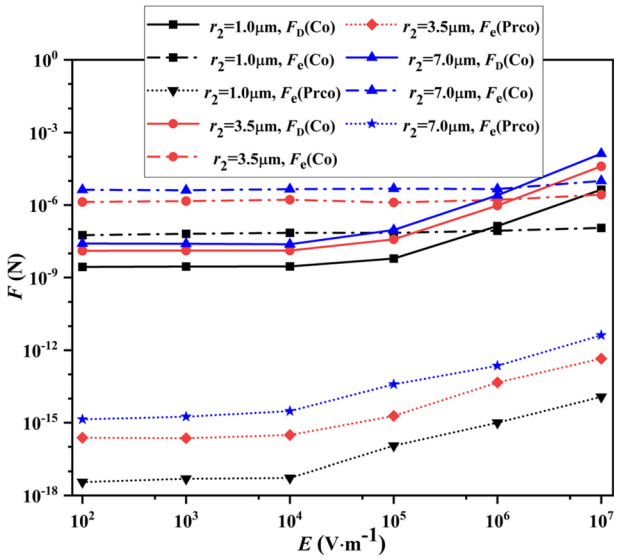

FIG. 6. The relation between the drag F_D and electrostatic force F_e of neutral droplet under different uniform electric fields. Among them, the charge ratio $CR = 1$ and charged droplet radius $r_1 = 10$ μm. Here, Co and Prco represent critical collision and pre-collision, respectively. The solid line and the dot dash line represent the drag and the electrostatic force at critical collision, respectively. The short dot line represents the electrostatic force before critical collision.

with the increase in the electric field, the collision efficiency under the same droplet size ratio first decreases and then rises slightly, and the internal causes of the changes in the two stages are different.

Based on the analysis of droplet relative motion trajectory and force, the variation characteristics of droplet collision efficiency except the vicinity of $E = 10^3$ V·m^{-1} and 10^4 V·m^{-1} can be explained as follows:

Normally, when only one of the two droplets is charged, the electrostatic force between the two droplets is always attractive. The charged droplet will accelerate its motion under the influence of the applied electric field force, and the disturbance around the droplet will be enhanced, which is not conducive to the collision between droplets. With the enhancement of the electric field, the disturbance flow is enhanced, which will offset the electrostatic attraction effect, so the collision efficiency under the same droplet size ratio decreases. At this stage, when the charged droplet has a larger charge (as *CR* increases), the electrostatic attraction between the two droplets can be effectively enhanced, thus effectively improving the possibility of droplet collision, as shown in Figs. 7(a), 7(c) and 7(d), 7(f). Moreover, as the neutral droplet size increases (β increases), the charge distribution area expands and more free charge can be accommodated. Consequently, the polarization effect will be more significant, and the electrostatic attraction between droplets will be enhanced (as shown in Fig. 6), so the droplet collision will be promoted, as shown in Figs. 7(a), 7(b) and 7(d), 7(e).

When the electric field is about above than 10^5 V·m^{-1}, the electrostatic attraction between droplets no longer dominates. The electric field is large enough at this time, so that the velocity of the charged droplet under its influence is relatively high, and the inertia effect is prominent and dominates. As shown in Figs. 7(g)–7(i), the collision of

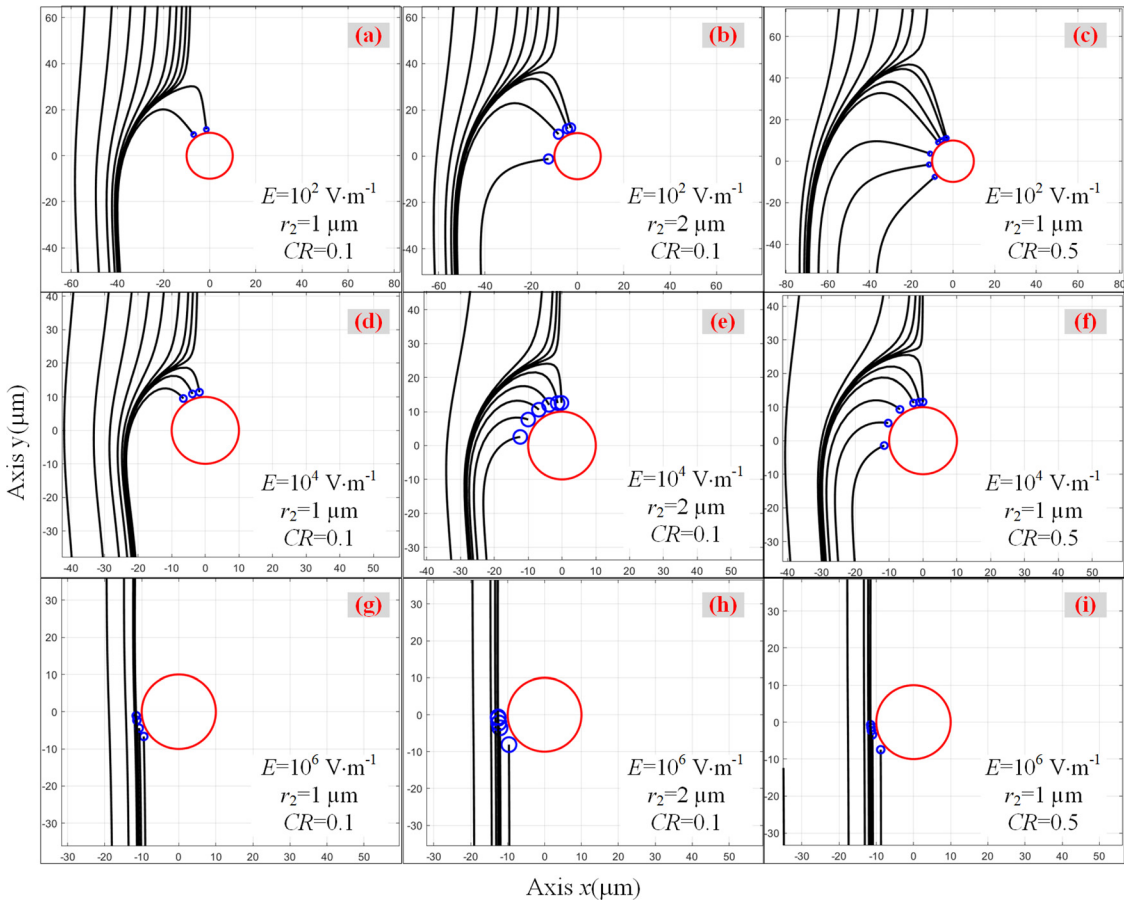

FIG. 7. The relative motion trajectory of a $r_1 = 10\ \mu$m charged droplet (red circle) and a neutral droplet (blue circle) under uniform vertical downward electric fields of values (a)–(c) $E = 10^2$ V·m^{-1}, (d)–(f) $E = 10^4$ V·m^{-1}, and (g)–(i) $E = 10^6$ V·m^{-1}. The neutral droplet radius is $r_2 = 1\ \mu$m for (a), (c), (d), (f), (g), and (i); and $r_2 = 2\ \mu$m for (b), (e), and (h). The charge ratio is $CR = 0.1$ for (a), (b), (d), (e), (g), and (h); and $CR = 0.5$ for (c), (f), and (i). Here, CR ($=Q/Q_{max}$) is the ratio of the charged droplet's actual charge to its maximum charge Q_{Ray}.

two droplets at this time is similar to vertical collision. With the increase in the electric field ($E > 10^5$ V·m^{-1}), the inertial effect is enhanced, partially offsetting the disturbance influence; hence, the collision efficiency rises somewhat and finally approaches 1.0.

For two neutral droplets, increasing the electric field strengthens polarization and raises the electrostatic force, facilitating collisions. Unlike charged droplets, neutral droplets are unaffected by external electric field force F_{AF}, avoiding the accelerated motion that disrupts collisions. Thus, collision efficiency rises with the electric field, as shown in Fig. 5. In addition, when the electric field is small (about less than 10^5 V·m^{-1}), the neutral droplet polarization is not significant, and the electrostatic attraction between the two neutral droplet is small, so the collision efficiency is low.

To further clarify the specific range of electric fields where the collision efficiency decreases at large droplet size ratios, we calculate the collision efficiency at electric fields slightly less than 10^3 V·m^{-1} and slightly more than 10^4 V·m^{-1}, as shown in Fig. 8. Furthermore, the disturbance velocity of neutral droplet varying with its size under the electric field $E = 10^3$ V·m^{-1} and 10^4 V·m^{-1} was calculated, so as to explore the internal reason why the collision efficiency of charged droplet and neutral droplet decreased when the droplet size ratio was large, as shown in Fig. 9.

As can be seen from Fig. 8, when the electric field is about 7.5×10^2 V·m^{-1} to 7.5×10^4 V·m^{-1}, the collision efficiency of charged droplet with high charge and neutral droplet has an inflection point with the increase in droplet size ratio β. The results can be explained as follows:

At this stage ($E = 7.5 \times 10^2$ V·m^{-1} to 7.5×10^4 V·m^{-1}), although the electrostatic attraction between the two droplets is dominant, the influence of disturbance flow is gradually prominent, and the inertial effect has not yet appeared, that is, a transitional stage. At the stage before the inflection point, the influence of disturbance has not been prominent, and the reason for the increase in collision efficiency with the increase in the droplet size ratio is the same as before. In other words, when the neutral droplet size is larger, the polarization effect inside the droplet will be more significant, and the electrostatic attraction will be enhanced. At the same time, when the droplet size ratio β is small, the disturbance velocity of neutral droplet does not increase

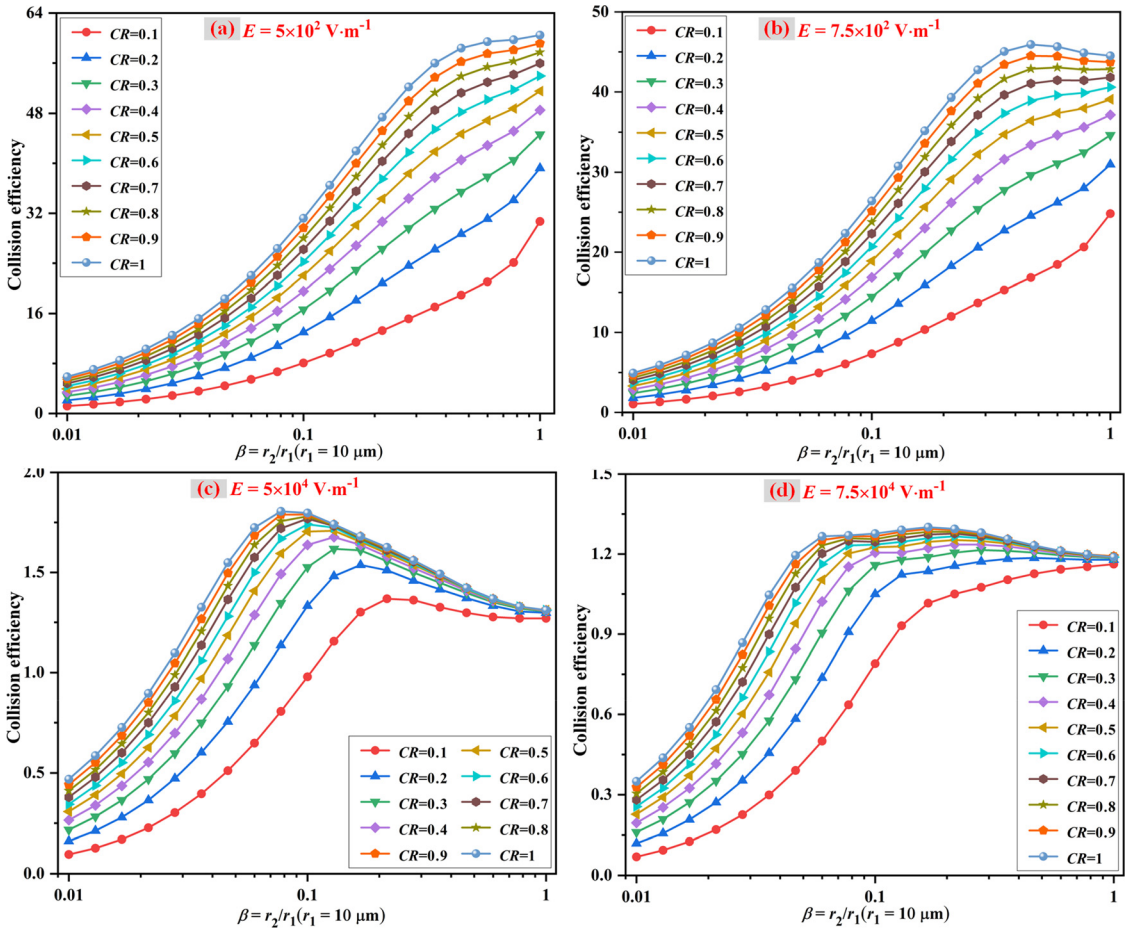

FIG. 8. Effects of β and CR on the collision efficiency when E is slightly less than 10^3 V·m^{-1} and slightly more than 10^4 V·m^{-1}, with charged droplet radius $r_1 = 10\ \mu$m. (a)–(d) The change of electric field intensity from 5×10^2 to 7.5×10^4 V·m^{-1}. Here, β ($=r_2/r_1$) is the radius ratio of neutral and charged droplets. CR ($=Q/Q_{max}$) is the ratio of the charged droplet's actual charge to its maximum charge Q_{Ray}.

significantly with the increase in the droplet size ratio β (as shown in Fig. 9), that is, the disturbance effect does not significantly offset the electrostatic attraction effect. In the later stage, when the droplet size is relatively large, the disturbance velocity increases significantly with the increase in droplet size ratio β. In addition, when the charge ratio CR is high, the droplet disturbance increases more significantly when the droplet size ratio β is large, as shown in the comparison between black and red dots or blue and yellow dots in Fig. 9.

The significant disturbance flow effects of high charge ratio CR and large droplet size ratio β offset the effects of electrostatic attraction, while the inertial effect does not appear to suppress the decrease in collision efficiency. Therefore, in the later stage, when the charged droplet charge and droplet size ratio are high, the collision efficiency will decrease with the increase in the droplet size ratio.

In fact, the electrostatic force of the charged droplet is influenced by both the charge ratio CR and the applied electric field E. Under the same electric field, the charged droplet with a higher charge ratio is subjected to a greater applied electric field force. Therefore, the charged droplet has a more obvious accelerated motion, resulting in enhanced disturbance around the droplet. Additionally, as the size of the neutral droplet increases, its drag force F_D also rises, which hinders droplet collision. As shown in Fig. 6 or Eq. (4), with increasing droplet size, both the maximum cross section A and the drag force F_D of the neutral droplet increase.

Finally, we investigated the relationship between the size of charged and neutral droplets and their collision efficiency under the same electric field strength ($E = 10^4$ V·m^{-1}) and charge ratio ($CR = 0.5$), as shown in Fig. 10. It can be seen that for various size combinations, the peak value of the collision efficiency approximately occurs when the two droplet sizes are close and the size of the neutral droplet is slightly smaller than that of the charged droplet.

B. Collision kernel characteristic

To characterize the frequency of droplet collision under different electric fields, the collision kernel was calculated. As shown in Fig. 11, under the same electric field, the collision kernel increases with the charge ratio CR. Similarly, for a fixed CR, the collision kernel grows

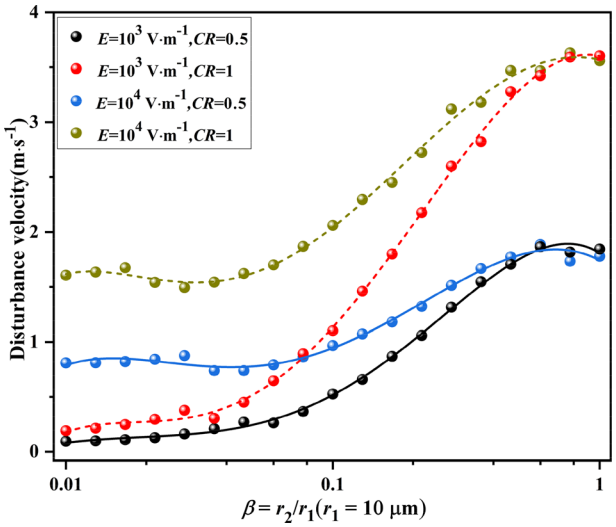

FIG. 9. Effect of neutral droplet size on its disturbance velocity at critical collision, with charged droplet radius $r_1 = 10\ \mu$m. Black and red dots represent the neutral droplet disturbance velocity at $E = 10^3$ V·m^{-1}, while blue and yellow dots represent it at $E = 10^4$ V·m^{-1}. The curves are fitting curves. The solid curve corresponds to $CR = 0.5$, and the dashed curve to $CR = 1$. Here, β ($=r_2/r_1$) is the radius ratio of neutral and charged droplets. CR ($=Q/Q_{max}$) is the ratio of the charged droplet's actual charge to its maximum charge Q_{Ray}.

with the electric field. According to Eq. (3), the collision kernel is mainly determined by the relative velocity difference $|V_1 - V_2|$ between the two droplets and the collision efficiency α. In fact, the second determinant of the collision kernel is actually the maximum horizontal distance r_{max} between two droplets that can collide, as the

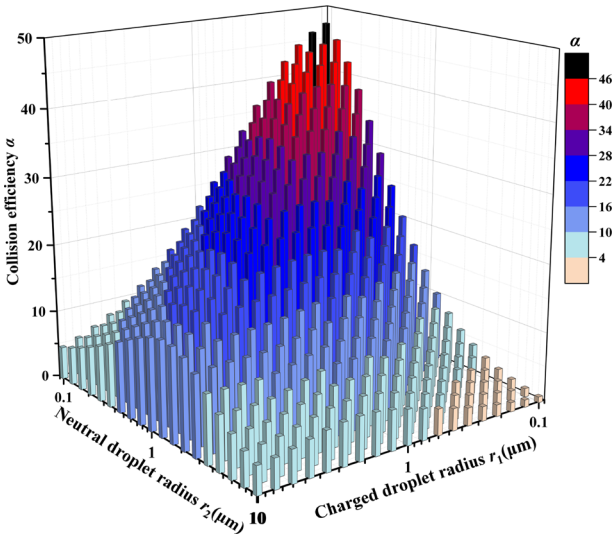

FIG. 10. Collision efficiency for charged-neutral droplet pairs of different radii, with the electric field $E = 10^4$ V·m^{-1} and charge ratio $CR = 0.5$. Here, CR ($=Q/Q_{max}$) is the ratio of the charged droplet's actual charge to its maximum charge (Rayleigh limit charge Q_{Ray}).

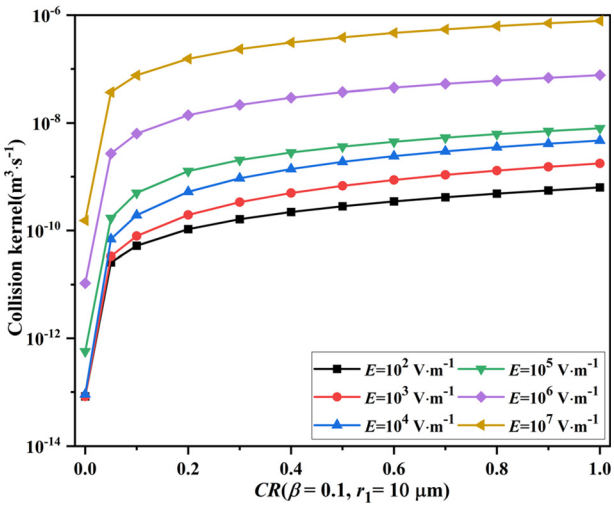

FIG. 11. Effects of CR on the collision kernel, with a set of uniform electric fields varying from 10^2 to 10^7 V·m^{-1}, with two droplets radius $r_1 = 10\ \mu$m and $r_2 = 1\ \mu$m, respectively. Here, CR ($=Q/Q_{max}$) is the ratio of the charged droplet's actual charge to its maximum charge Q_{Ray}. β ($=r_2/r_1$) is the radius ratio of neutral and charged droplets.

collision kernel $K = \alpha\ |\boldsymbol{V_1} - \boldsymbol{V_2}|\ \pi\ (r_1 + r_2)^2 = |\boldsymbol{V_1} - \boldsymbol{V_2}|\ \pi\ (r_{max})^2$. When the charge ratio CR is larger, on the one hand, the electrostatic attraction between the two droplets will increase, which can effectively promote the occurrence of collision. On the other hand, the applied electric field force on the charged droplet ($CR > 0$) will increase, which can effectively enhance its velocity. Therefore, under the same electric field, a higher charge ratio CR leads to a greater maximum horizontal distance and velocity difference, resulting in a higher collision kernel.

When the applied electric field increases, although the collision efficiency (or the maximum horizontal distance r_{max}) of charged and neutral droplets decreases, the velocity of charged droplet rises significantly. The increase in the velocity difference $|\boldsymbol{V_1} - \boldsymbol{V_2}|$ is more significant than the decrease in the maximum horizontal distance r_{max}. Therefore, at the same charge ratio CR, the collision kernel continues to increase with the applied electric field. Additionally, the collision kernel of two neutral droplets ($CR = 0$) is much lower than that of the charged and neutral droplets under the same electric field, as neutral droplets do not accelerate the motion under the applied electric field force F_{AE} like charged droplets.

As shown in Fig. 12, the effects of droplet size ratio β and charge ratio CR on collision kernel under various electric fields are specifically presented. The results show that the collision kernel of each applied electric field (from 10^2 V·m^{-1} to 10^7 V·m^{-1}) increases with the increase in the droplet size ratio β under the same charge ratio CR. It can also be seen that under the same droplet size ratio β, the collision kernel of each applied electric field increases with the increase in the charge ratio CR.

As mentioned earlier, the collision kernel is mainly determined by the relative velocity difference $|V_1 - V_2|$ and the maximum horizontal distance r_{max} between two droplets that can collide. Under the same charge ratio CR, the increase in the droplet size ratio β has little effect on the velocity difference $|V_1 - V_2|$ of the two droplets. It is mainly reflected that the large neutral droplet

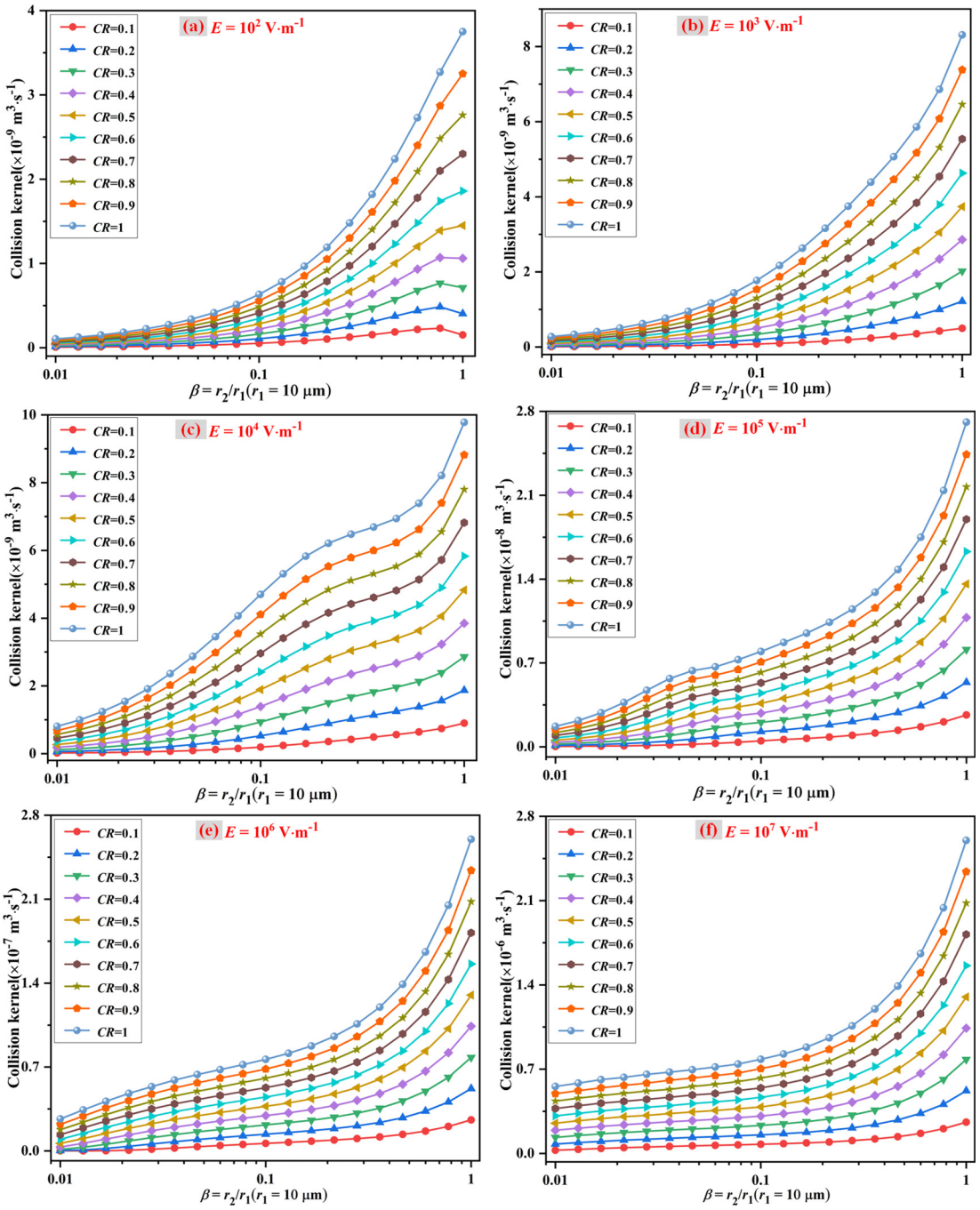

FIG. 12. Effects of β and CR on the collision kernel, with charged droplet radius $r_1 = 10\ \mu m$. (a)–(f) The collision kernel of a charged-neutral droplet pair when the electric field intensity E varying from 10^2 to 10^7 V·m^{-1}. Here, β ($=r_2/r_1$) is the radius ratio of neutral and charged droplets. CR ($=Q/Q_{max}$) is the ratio of the charged droplet's actual charge to its maximum charge Q_{Ray}.

has more obvious polarization effect, which enhances the electrostatic force between the two droplets and causes the increase in the maximum horizontal distance r_{max}. As shown in Fig. 3, except for Figs. 3(b) and 3(c), the collision efficiency α increases with the increase in the droplet size ratio β under each electric field. For the transition stage of 7.5×10^2 V·m^{-1} to 7.5×10^4 V·m^{-1} electric fields in Figs. 3(b) and 7(c), Figs. 8(b) and 8(c), although the collision efficiency α decreases with the increase in the droplet size ratio

β in the later stage, r_{max} that actually determines the collision kernel increases, so the collision kernel will also increase.

Finally, we investigated the relationship between the size of charged and neutral droplets and their collision kernel under the same electric field strength ($E = 10^4$ V·m^{-1}) and charge ratio ($CR = 0.5$), as shown in Fig. 13. It can be seen that the larger the sizes of the two droplets, the more beneficial it is for the enhancement of the collision kernel, and the peak appears when the sizes of both droplets are larger.

IV. CONCLUSIONS

In this paper, a computational model is proposed to study the collision characteristics of two neutral droplets or a neutral droplet and a charged droplet with varying charge ratios (particularly at high charges near the Rayleigh limit) under different electric field strengths. The collision characteristics are characterized by collision efficiency and collision kernel, which reflect the probability and frequency of droplet collisions, respectively. The results are shown as follows:

(i) Collision efficiency at extremely low and high electric fields:
The collision efficiency increases with the droplet size ratio (specifically, it is size of the neutral droplet) under extremely low electric fields (near 10^2 V·m^{-1}) and high electric fields (ranging from 7.5×10^4 to 10^7 V·m^{-1}). Furthermore, in extremely low electric fields, the enhancement of collision efficiency shows no apparently upper limit, while under high electric fields, the collision efficiency plateaus, ultimately stabilizing around 1.0.

(ii) Collision efficiency in transition stage:
In contrast, at moderate electric fields (ranging from 7.5×10^2 to 7.5×10^4 V·m^{-1}), a transition stage is observed. In this stage, the disturbance influence is continuously enhanced, while the inertia effect is not shown. Here, there is a peak in the collision efficiency of highly charged droplet (especially near the Rayleigh limit) with neutral droplet as the droplet size ratio increases.

(iii) Collision efficiency over the entire electric field range:
Within the electric field range of 10^2 to 10^7 V·m^{-1}, increasing the charge of the charged droplet enhances the collision efficiency of the charged-neutral droplet pair. For a given droplet size ratio, the collision efficiency of micron-sized charged-neutral droplet pairs initially decreases with increasing electric field due to the disturbance effect and then rises slightly to about 1.0 due to the inertial effect. For two neutral droplets ($CR = 0$), the collision efficiency first increases slowly and then rises sharply as the electric field strength increases. When the electric field $E > 5 \times 10^5$ V·m^{-1}, the collision efficiency of two neutral droplets surpasses that of the charged-neutral droplet pair. However, at electric field strengths below 10^5 V·m^{-1}, the collision efficiency of two neutral droplets is very low.

(iv) Collision kernel over the entire electric field range:
The collision kernel increases with the droplet size ratio (specifically, it is size of the neutral droplet) across all studied electric field strengths (10^2 V·m^{-1} to 10^7 V·m^{-1}). Moreover, the increase in the applied electric field can significantly increase the collision kernel of neutral droplets or a charged-neutral droplet pair. The collision kernel of two neutral droplets is much smaller than that of the charged and neutral droplets under the same electric field. It is expected that even with electric fields exceeding 5×10^5 V·m^{-1}, neutral droplets will take a considerable amount of time to collide and coalesce into larger droplets.

(v) Effect of droplet size on collision characteristics:
The peak collision efficiency occurs when the droplet sizes are close, with the neutral droplet slightly smaller than the charged one, and the collision kernel is enhanced as the droplet sizes increase, peaking when both droplets are larger.

The research results are crucial for understanding the internal physical processes of cloud droplet collisions under different uniform electric fields and varying charges (especially high charges). Future studies could consider the effect of electric field intensity on the evolution of droplet size distribution and the effect of electric field heterogeneity on droplet collision characteristics.

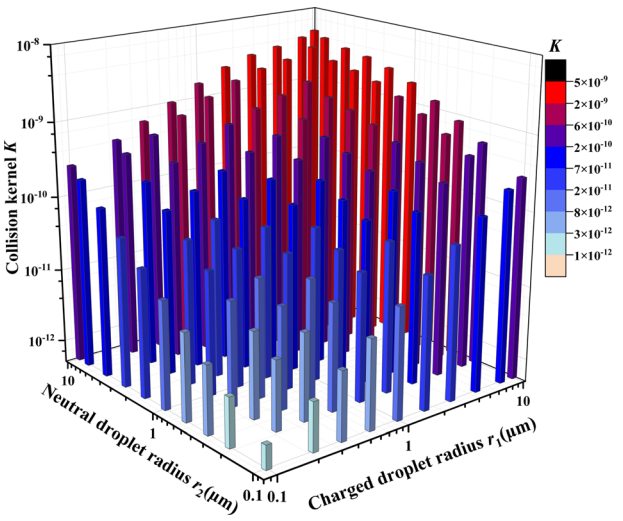

FIG. 13. Collision kernel for charged-neutral droplet pairs of different radii, with the electric field $E = 10^4$ V·m^{-1} and charge ratio $CR = 0.5$. Here, CR ($=Q/Q_{max}$) is the ratio of the charged droplet's actual charge to its maximum charge (Rayleigh limit charge Q_{Ray}).

ACKNOWLEDGMENTS

This work is supported by the National Natural Science Foundation of China (Grant Nos. 52207158).

AUTHOR DECLARATIONS

Conflict of Interest

The authors have no conflicts to disclose.

Author Contributions

Ming Zhang: Conceptualization (equal); Investigation (equal); Methodology (equal); Writing – review & editing (equal). **Zhiwen Yang:** Conceptualization (equal); Formal analysis (equal); Methodology (equal); Validation (equal); Writing – original draft (equal). **Chuan Li:** Conceptualization (equal); Funding acquisition (equal); Writing – review & editing (equal). **Jiawei Li:**

Conceptualization (equal); Formal analysis (equal); Investigation (supporting). **Dingchen Li:** Conceptualization (supporting); Writing – review & editing (equal). **Qixiong Fu:** Conceptualization (supporting). **Kexun Yu:** Conceptualization (supporting).

DATA AVAILABILITY

The data that support the findings of this study are available from the corresponding author upon reasonable request.

REFERENCES

[1]A. Jaworek, A. M. Ganan-Calvo, and Z. Machala, "Low temperature plasmas and electrosprays," J. Phys. D: Appl. Phys. **52**, 233001 (2019).

[2]W. Tong, H. Li, D. Liu, Y. Wu, M. Xu, and K. Wang, "Study on the changes in the reverse recovery characteristics of high-power thyristor under 14.1 MeV fusion neutron irradiation," Fusion Eng. Des. **211**, 114744 (2025).

[3]A. M. L. D. Rio, R. S. Aparicio-Garcia, A. G. J. Gracia, and R. V. Arreguin, "Evaluation and analysis of fog dispersion under the influence of an electric field," in *20th International Symposium On Electrical Apparatus and Technologies (SIELA)* (IEEE, 2018), pp. 1–4.

[4]M. Zhang, J. Li, C. Li, F. He, D. Li, K. Yu, and Y. Pan, "Investigation of the effects of parallel electric field on fog dissipation," J. Phys. D: Appl. Phys. **56**, 375204 (2023).

[5]W. Zheng, H. Ma, M. Zhang, F. Xue, K. Yu, Y. Yang, S. Ma, C. Wang, Y. Pan, Z. Shu, J. Mu, W. Yang, and X. Yin, "Evaluation of the first negative ion-based cloud seeding and rain enhancement trial in China," Water **13**, 2473 (2021).

[6]Y. Yang, H. Chen, C. Li, and P. Wang, "Ion induced nucleation of charged droplets enhanced by external electric field," Phys. Plasmas **31**, 073505 (2024).

[7]S. Guo and H. Xue, "The enhancement of droplet collision by electric charges and atmospheric electric fields," Atmos. Chem. Phys. **21**, 69–85 (2021).

[8]G. Magnusson, A. Dubey, R. Kearney, G. P. Bewley, and B. Mehlig, "Collisions of micron-sized charged water droplets in still air," Phys. Rev. Fluids **7**, 043601 (2022).

[9]H. R. Pruppacher and J. D. Klett, *Microphysics of Clouds and Precipitation* (Dordrecht: Kluwer Academic Publishers, 1997).

[10]D. A. Stewart and O. M. Essenwanger, "A survey of fog and related optical propagation characteristics," Rev. Geophys. **20**, 481–495, https://doi.org/10.1029/RG020i003p00481 (1982).

[11]K. V. Beard, I. D. Russell, and H. T. Ochs III, "Coalescence efficiency measurements for minimally charged cloud drops," J. Atmos. Sci. **59**, 233–243 (2002).

[12]B. A. Tinsley, R. P. Rohrbaugh, M. Hei, and K. V. Beard, "Effects of image charges on the scavenging of aerosol particles by cloud droplets and on droplet charging and possible ice nucleation processes," J. Atmos. Sci. **57**, 2118–2134 (2000).

[13]Y. Yang, S. Yang, C. Li, Y. Wang, X. Pi, Y. Lu, and R. Wu, "Insulator defect detection under extreme weather based on synthetic weather algorithm and improved YOLOv7," High Volt. **10**, 000000 (2025).

[14]S. N. Grover, "A numerical determination of the effect of electric fields and charges on the efficiency with which cloud drops and small raindrops collide with aerosol particles," Pure Appl. Geophys. **114**, 509–520 (1976).

[15]D. Cruzat and C. Jerez-Hanckes, "Electrostatic fog water collection," J. Electrostat. **96**, 128–133 (2018).

[16]A. Khain, V. Arkhipov, M. Pinsky, Y. Feldman, and Y. Ryabov, "Rain enhancement and fog elimination by seeding with charged droplets. Part I: Theory and numerical simulations," J. Appl. Meteorol. **43**, 1513–1529 (2004).

[17]M. Damak and K. K. Varanasi, "Electrostatically driven fog collection using space charge injection," Sci. Adv. **4**, eaao5323 (2018).

[18]D. Li, C. Li, M. Xiao, J. Li, Z. Yang, Q. Fu, M. Zhang, K. Yu, and Y. Pan, "Deconstructing plasma fog collection technology: An experimental study on factors impacting collection efficiency," J. Phys. D: Appl. Phys. **57**, 075201 (2024).

[19]D. Li, C. Li, M. Zhang, M. Xiao, J. Li, Z. Yang, Q. Fu, P. Wang, K. Yu, and Y. Pan, "Advanced fog harvesting method by coupling plasma and micro/nano materials," ACS Appl. Mater. Interfaces **16**, 10984–10995 (2024).

[20]R. G. Semonin and H. R. Plumlee, "Collision efficiency of charged cloud droplets in electric fields," J. Geophys. Res. **71**, 4271–4278, https://doi.org/10.1029/JZ071i018p04271 (1966).

[21]P. Wang, C. Li, M. Zhang, J. Li, Z. Liu, Y. Yang, K. Yu, and Y. Pan, "Synergistic effect of charges and electric field: Water droplet condensation and coalescence in a sub-saturated cloud chamber," Plasma Sources Sci. Technol. **29**, 045005 (2020).

[22]J. Li, C. Li, P. Wang, F. He, M. Xiao, M. Zhang, Y. Yang, K. Yu, and Y. Pan, "Numerical analysis of collision characteristics between charged drop and neutral droplet under uniform electric field," J. Phys. D: Appl. Phys. **54**, 455201 (2021).

[23]M. H. Davis, "Two charged spherical conductors in a uniform electric field: Forces and field strength," Q J. Mech. Appl. Math. **17**, 499–511 (1964).

[24]D. Duft, T. Achtzehn, R. Müller, B. A. Huber, and T. Leisner, "Coulomb fission: Rayleigh jets from levitated microdroplets," Nature **421**, 128 (2003).

[25]M. H. P. Ambaum, T. Auerswald, R. Eaves, and R. G. Harrisonet, "Enhanced attraction between drops carrying fluctuating charge distributions," Proc. Roy. Soc. A-Math. Phys. Eng. Sci. **478**, 20210714 (2022).

[26]L. Zhou, B. A. Tinsley, and A. Plemmons, "Scavenging in weakly electrified saturated and subsaturated clouds, treating aerosol particles and droplets as conducting spheres," J. Geophys. Res.-Atmos. **114**, 201–215, https://doi.org/10.1029/2008JD011527 (2009).

[27]D. C. Taflin, T. L. Ward, and E. J. Davis, "Electrified droplet fission and the Rayleigh limit," Langmuir **5**, 376–384 (1989).

[28]M. Pinsky, A. Khain, and M. Shapiro, "Collision efficiency of drops in a wide range of Reynolds numbers: Effects of pressure on spectrum evolution," J. Atmos. Sci. **58**, 742–764 (2001).

[29]T. Song, X. Xing, Y. Yang, X. Li, and R. Yang, "Study on the effect of sodium polyacrylate and its compounds on artificial warm fog dissipation," Adv. Mater. Res. **1052**, 226–230 (2014).

[30]L. P. Wang, O. Ayala, and W. W. Grabowski, "Improved formulations of the superposition method," J. Atmos. Sci. **62**, 1255–1266 (2005).

[31]Z. Wang, K. Dong, L. Tian, J. Wang, and J. Tu, "Numerical study on coalescence behavior of suspended drop pair in viscous liquid under uniform electric field," AIP Adv. **8**, 085215 (2018).

[32]L. F. Shampine and M. W. Reichelt, "The MATLAB ODE suite," SIAM J. Sci. Comput. **18**, 1–22 (1997).